



M2 - TSI

UE52 EARTH OBSERVATION REPORT

Infrastructure Development in Dubai

Author:
Arthur Scharf

March 3, 2017

1 Introduction

Dubai is a city located in the United Arab Emirates near the Persian Gulf and is well known and acknowledged as a global city. Since oil was discovered in the late 1906's, Dubai started to expand very fast. However, nowadays only about 5% of Dubai's revenue is connected to the black gold, but instead Dubai is known for financial services, tourism and aviation [Dubai, 2017-03-03]. Also, Dubai is known for having the world's tallest building, the Burj Khalifa and its extremely high living expenses. This leads to the question how, and in which way, Dubai has been expanding and growing since the late 1960's.

In this study the development of Dubai's infrastructure will be analysed by using satellite images within the visible bands / spectrum. Since analysing infrastructure from space in the visible spectrum is a difficult topic, this report will focus on two different methods: first, an analysis of the captured colours, i.e. water and land, by using supervised classification (kNN algorithm) and second, a pattern and structure analysis using edge detection techniques and morphological filtering.

To be able to analyse the actual development of structure, land and water evolution LandSat Data from since 1984 until 2016 will be used - one satellite image per year within the same or a close month, depending on the cloud conditions.

In particular, the following sections will cover the involved satellites and its instruments that are used to capture the images. Also, the images themselves will be looked closer at, especially regarding resolution, image period etc. After, the aforementioned methods and the overall analysis approach will be explained in more detail. The results of this analysis will then be discussed and a conclusion given, stating the findings and a future outlook on this particular topic of infrastructure development observation.

2 Satellite Instruments

Since this report covers a period of about 32 years, satellite imagery from different satellite platforms will be used. To ensure a minimum compatibility between the images, e.g. regarding resolution etc., images from the same satellite family will be used - in particular LandSat satellites 4, 5, 7 and 8. The LandSat project is a joint program of the U.S. Geological Survey and (USGS) and NASA, with the first satellite launch in 1972 [USGS, 2017-03-01a], to provide continuous global earth observation data coverage .

Even though the resolution is only moderate, the LandSat satellites provide a continuous and global coverage - resulting in a vast amount of image data that reaches back around 4 decades. The data is made publicly available for free within the Landsat remote sensing (LRS) component of USGS in the EROS data centre.[USGS, 2017-03-01b] A first initial screening of the image data that is available from LandSat-1 to LandSat-3 revealed very quickly that those image data

might not be very suitable for a proper analysis, since the very early LandSat satellites used Taperecorders to actually record images, so the retrieved resolution and image quality is not very much comparable to the later LandSat versions. Thus, LandSat-1 to LandSat-3 data is not used in the Analysis.

Also, for the purpose of this study, only the visible spectral bands are used in the image data. However, for the sake of completeness, the following subsections give an overview of all available spectral bands in the respective instruments.

2.1 LandSat-4 and 5 Thematic Mapper

LandSat-4 was a project by NASA, NOAA, EOSAT and USGS and was launched on 16th July 1982 on a Delta 3920 rocket. The satellite weighted about 1942kg and used a Hydrazine propulsion system for its attitude control system. The Communication System used S, X, L and Ku bands and had a data rate of about 85 Mbps on the downlink via the Tracking and Data Relay Satellite System (TDRSS). The satellite was launched in a sun-synchronous circular orbit with an inclination of 98.2° at a height of 705km [USGS, 2017-03-02a].

LandSat-4 and 5 were two identical satellites, with LandSat-5 being a backup satellite that outlived LandSat-4 and provided data until 2013 [Wikipedia, 2017-03-02; USGS, 2017-03-02b].

Both satellites carried two observation instruments, the Multispectral Scanner (MSS) and the Thematic Mapper (TM) with the following available spectral bands:

No.	Band	λ	resolution
Band 4	Visible	0.5 - 0.6 μm	57 x 79 m
Band 5	Visible	0.6 - 0.7 μm	57 x 79 m
Band 6	Near IR	0.7 - 0.8 μm	57 x 79 m
Band 7	Near IR	0.8 - 1.1 μm	57 x 79 m

Table 1: MSS Instrument on Landsat 4 and 5[USGS, 2017-03-02a][USGS, 2017-03-02b]

No.	Band	λ	resolution
Band 1	Visible	0.45 - 0.52 μm	30 m
Band 2	Visible	0.52 - 0.60 μm	30 m
Band 3	Visible	0.63 - 0.69 μm	30 m
Band 4	Near IR	0.76 - 0.90 μm	30 m
Band 5	Near IR	1.55 - 1.75 μm	30 m
Band 6	Thermal	10.40 - 12.50 μm	30 m
Band 7	Mid IR	2.08 - 2.35 μm	30 m

Table 2: TM Instrument on Landsat 4 and 5[USGS, 2017-03-02a,-]

2.2 LandSat-7 Enhanced Thematic Mapper Plus

LandSat-7, a successor to LandSat-4 and 5 since the launcher during the LandSat-6 launch failed, was launched on 15th April 1999 on a Delta II rocket. This satellite was heavier than its predecessors with about 2200kg and used a more sophisticated downlink method (Solid State Recorders or SSR's) to provide an improved downlink speed of 150Mbps.

The satellite was launched the same sun-synchronous circular orbit as LandSat-4 with an inclination of 98.2° at a height of 705km, but with about 15 minutes behind LandSat-4 [USGS, 2017-03-02c].

Another improvement was done on the Thematic Mapper, here called the Enhanced Thematic Mapper Plus (ETM+), with an increased amount of spectral bands and a panchromatic band with double the resolution compared to the other ones. Table 3 shows a quick overview over the available spectral bands.

No.	Band	λ	resolution
Band 1	Visible	0.45 - 0.52 μm	30 m
Band 2	Visible	0.52 - 0.60 μm	30 m
Band 3	Visible	0.63 - 0.69 μm	30 m
Band 4	Near IR	0.76 - 0.90 μm	30 m
Band 5	Near IR	1.55 - 1.75 μm	30 m
Band 6	Thermal	10.40 - 12.50 μm	60 m Low & High Gain
Band 7	Mid IR	2.08 - 2.35 μm	30 m
Band 8	Panchromatic	0.52 - 0.90 μm	15 m

Table 3: ETM+ Instrument on Landsat 7[USGS, 2017-03-02c]

2.3 LandSat-8 Operational Land Imager

LandSat-8 was another iteration of the LandSat family and was launched on February 11, 2013 on an Atlas-V rocket. Again, this satellite was heavier compared to its predecessors with a weight of 2623kg. Contrary to LandSat-7, two distinct imaging instruments were used, the Operational Land Imager (OLI) and the Thermal Infrared Sensor (TIRS), where the OLI instruments was essentially the ETM+ with an additional detector to observe Cirrus clouds [USGS, 2017-03-02c]. The tables 4 and 5 show the appropriate spectral band properties for both instruments.

3 Satellite Imaginary and Observations

As explained in the previous chapter, imagery provided by different satellites and satellite instruments were used in this report. This chapter will give a short overview on the used image

No.	Band	λ	resolution
Band 1	Visible	0.43 - 0.45 μm	30 m
Band 2	Visible	0.45 - 0.51 μm	30 m
Band 3	Visible	0.53 - 0.59 μm	30 m
Band 4	Red	0.64 - 0.67 μm	30 m
Band 5	Near IR	0.85 - 0.88 μm	30 m
Band 6	SWIR 1	1.57 - 1.65 μm	30 m
Band 7	SWIR 2	2.11 - 2.29 μm	30 m
Band 8	Panchromatic	0.52 - 0.90 μm	15 m
Band 8	Cirrus	1.36 - 1.38 μm	30 m

Table 4: OLI Instrument on Landsat 8 [?]

No.	Band	λ	resolution
Band 10	TIRS 1	10.6 - 11.19 μm	100 m
Band 11	TIRS 2	11.5 - 12.51 μm	100 m

Table 5: TIRS Instrument on Landsat 8 [?]

and their properties. All Images were selected and downloaded via the *EarthExplorer*, a tool provided by the USGS to select earth observation data based on different criteria, such as coordinates (Degree/Minute/Second or WRS-2¹), different features in the images and data ranges. Also, different data sets provided by different programmes and satellites can be searched [Explorer, 2017-03-02].

3.1 LandSat-4 TM Imagery

Image Number	Resolution	Band	Capture Year	Location
LT41600431988027XXX03.jpg	30 m / pixel	Visible	1988	160/043 (WRS-2)
LT41600431990240XXX03.jpg	30 m / pixel	Visible	1990	160/043 (WRS-2)
LT41600431992166XXX02.jpg	30 m / pixel	Visible	1992	160/043 (WRS-2)

3.2 LandSat-5 TM Imagery

For reasons unknown LandSat-5 acquired only very few data during the period of 1998 and 2008 - while researching this interesting data gap it could not be determined if this gap was due to problems or introduced on purpose. However, the MSS, the second instrument on board was

¹World-Reference-System-2 for LandSat satellites consisting of two numbers, the Path and the Row of the satellite ground track

Image Number	Resolution	Band	Capture Year	Location
LT51600431984136XXX12.jpg	30 m / pixel	Visible	1984	160/043 (WRS-2)
LT51600431985042AAA04.jpg	30 m / pixel	Visible	1985	160/043 (WRS-2)
LT51600431986045XXX05.jpg	30 m / pixel	Visible	1986	160/043 (WRS-2)
LT51600431987272XXX10.jpg	30 m / pixel	Visible	1987	160/043 (WRS-2)
LT51600431989165ISP00.jpg	30 m / pixel	Visible	1989	160/043 (WRS-2)
LT51600431991171ISP00.jpg	30 m / pixel	Visible	1991	160/043 (WRS-2)
LT51600431993160ISP00.jpg	30 m / pixel	Visible	1993	160/043 (WRS-2)
LT51600431994179ISP00.jpg	30 m / pixel	Visible	1994	160/043 (WRS-2)
LT51600431995278ISP00.jpg	30 m / pixel	Visible	1995	160/043 (WRS-2)
LT51600431996345ISP00.jpg	30 m / pixel	Visible	1996	160/043 (WRS-2)
LT51600431997011ISP00.jpg	30 m / pixel	Visible	1997	160/043 (WRS-2)
LT51600431998286XXX01.jpg	30 m / pixel	Visible	1998	160/043 (WRS-2)
LT51600432008138KHC01.jpg	30 m / pixel	Visible	2008	160/043 (WRS-2)

powered off in 1999 and then powered back on in 2013, after the TM instrument failed [USGS, 2017-03-02b].

3.3 LandSat-7 ETM+ Imagery

Image Number	Resolution	Band	Capture Year	Location
LE71600431999265SGS01.jpg	30 m / pixel	Visible	1999	160/043 (WRS-2)
LE71600432000188SGS00.jpg	30 m / pixel	Visible	2000	160/043 (WRS-2)
LE71600432001190EDC00.jpg	30 m / pixel	Visible	2001	160/043 (WRS-2)
LE71600432002273SGS01.jpg	30 m / pixel	Visible	2002	160/043 (WRS-2)
LE71600432003148ASN00.jpg	30 m / pixel	Visible	2003	160/043 (WRS-2)

In 2003 the Scan Line Correction (SLC) feature of the ETM+ instrument failed, which led to disturbed images due to the fact that the instrument did not correct the movement of the satellite in orbit while taking images. Due to the heavy image distortion in the area this report is actually focused on (coast of the Emirates, see upper left part of fig. 1), this data is discarded for the use within this study, even though image data would be available up until the present day [USGS, 2017-03-02c].

3.4 LandSat-8 OLI Imagery

Since the Images provided by LandSat-7 provided after 2003 were not usable, and LandSat-5 was decommissioned in 2013 [USGS, 2017-03-02b], the most recent data was selected from LandSat-8. This was done in particular since the resolution and image capture location and

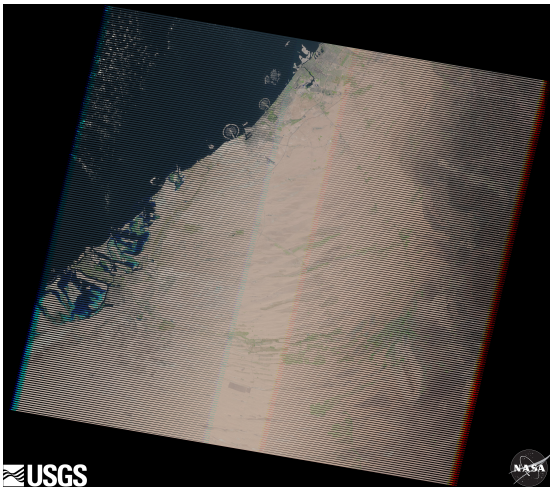


Figure 1: L-7 ETM+ SLC OFF (2010)

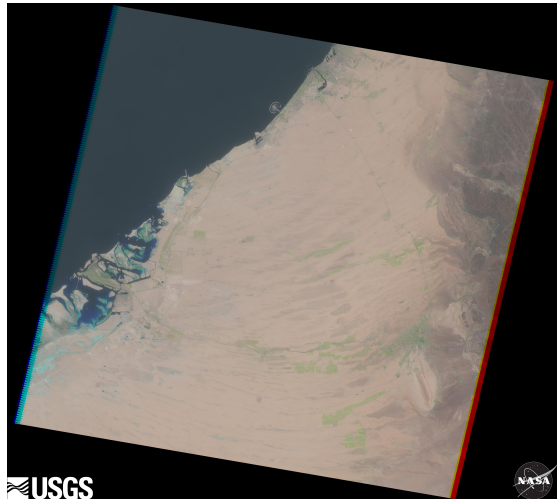


Figure 2: L-7 ETM+ SLC ON (2003)

orientation is the same as in the previous pictures, even though for this time period newer and high-resolution satellite images would be available. This significantly decreases the effort for the analysis part of this report.

Image Number	Resolution	Band	Capture Year	Location
LC81600432013151LGN00.jpg	30 m / pixel	Visible	2013	160/043 (WRS-2)
LC81600432014154LGN00.jpg	30 m / pixel	Visible	2014	160/043 (WRS-2)
LC81600432015269LGN00.jpg	30 m / pixel	Visible	2015	160/043 (WRS-2)
LC81600432016352LGN00.jpg	30 m / pixel	Visible	2016	160/043 (WRS-2)

4 Analysis Methods

After having obtained the relevant images as explained in the previous chapter, the image data had to be processed. For this report in particular, the focus was put on the analysis of the structure that is present in the region of interest (ROI) of the image. Under the assumption that a civilisation that is expanding in an area with enough free space available in the surrounding (as is the case in the quite desert-like area around Dubai), will build houses, roads and other periphery that is required to sustain a civilisation, the hypothesis for image analysis is as follows,

The more edges and/or junctions are detected the higher the development level of infrastructure.

Another assumption that can be made concerning infrastructure development is, that if a city grows, the natural flora and fauna is reduced. This leads to a second hypothesis that can be made.

The less water (sea, rivers, lakes) and vegetation is observed the higher the development level of infrastructure.

To prove these hypotheses, various methods and techniques have been used, as will be explained in the following sub-chapters.

4.1 Preprocessing

Since the data gathered from *EarthExplorer* has already been preprocessed, i.e. assembled from different visible spectra, corrected w.r.t. north and watermarked, it needed some initial preprocessing. Also, since the images were not equal in pixel size and did not feature the Region-of-Interest in the same pixel area, a machine-based pre-processing was not feasible in the scope of this project. Thus, all images were edited using a mask of the current borders of Dubai, c.f. fig. 3. This was done by masking the borders on the latest 2016-image of LandSat-8, which corresponds the best to the Google-Maps Image (note: fig. 3 contains Dubai City and Greater Dubai, for the purpose of this report Greater Dubai borders were used). Since, as mentioned, the image sizes did not match and the ROI location varied, the mask was adjusted for every image manually using Photoshop (see e.g. fig. 4) by overlaying the border mask. As a result each image had a correctly masked Region-of-Interest. An example image is shown in fig. 5).

Having obtained the actual area/region of interest, the image was cropped to include as little overhead pixels as possible to reduce the image size and thus the processing time and effort. Also, cropping the image made it possible to equalise the size of images in terms of pixel width and height. This process is visualised between figs. 5 and 6. The cropped images were now reduced to a size of 3201x3001 pixels, and the white background was converted to black for easier processing in later stages.

During the screening of the images it was also very obvious, that the brightness and colours had significant variation between different pictures. This would vastly affect the analysis w.r.t. to the second hypothesis. This is the reason why the histograms of the images were equalised with the built-in MATLAB function `imhistmatch`, so that the brightness and colour would match very well in between different images. It was possible to do so, since the images featured the exact same region of interest. The result of this histogram equalisation performed on fig. 6 can be seen in fig. 7. The cropping (selecting the ROI) and histogram equalisation was done automatically using Matlab, see appendix A.

4.2 Structure Detection

The now masked, cropped and equalised images could then be used for machine based processing. To prove or disprove the first hypotheses, the MATLAB built-in edge detection was used with some morphological filters.



Figure 3: Borders of Dubai marked in Red[Maps, 2017-03-02]

First, the images are grayscaled with the MATLAB function `rgb2gray` (fig. 8), then an edge-detection was performed with `edge` on the grayscaled image (fig. 9). Looking at the image resulting from this step, it can be seen that also the borders at the masked area are detected, which is not desired because we are not interested in the mask border. To remove the outer detected edges, a morphologic erosion is performed with the parameter of 1 pixel (meaning only 1 pixel will be eroded) (fig. 11).

Since the edge detection only detected the edges, and not for example the inner part of a rectangle (assuming the rectangle being a house, or street), a morphological closing was performed to close those inner parts with a logical 1 (fig. 10) (corresponding to the white colour in the binary images). Different edge detection algorithms were tested, e.g. Canny, but the build-in edge function provided the best results in terms of detecting the desired features (mostly streets/houses etc.). Also, the parameters for the morphological closing were chosen as *Infinite*, since

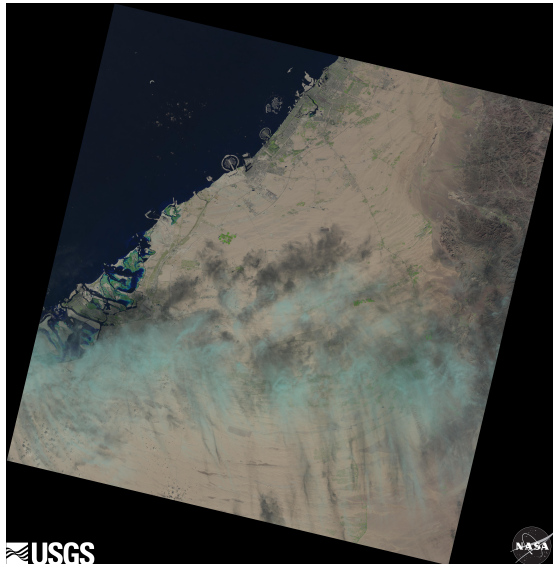


Figure 4: L-8 OLI Image (2016)



Figure 5: L-8 OLI Image (2016) masked (ROI)



Figure 6: L-8 OLI Image (2016) cropped

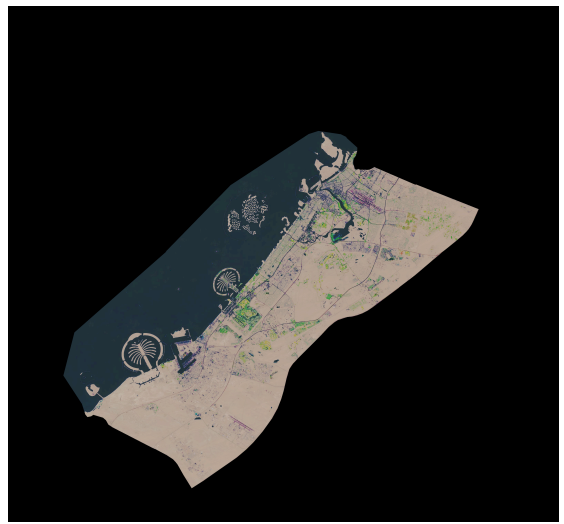


Figure 7: L-8 OLI Image (2016) equalized

a complete closure of the inner areas was desired.

After having obtained the masked area corresponding to streets, houses and other structured elements, the area could be calculated by simply summing the binary image.

4.3 Colour Analysis

To obtain images that support or do not support the second hypothesis, a colour analysis of the image was necessary. As explained in section 4.1, the histograms of each distinct image

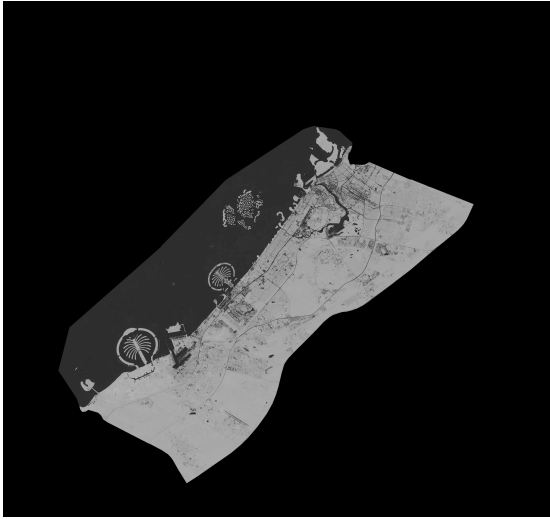


Figure 8: L-8 OLI Image (2016) grayscaled

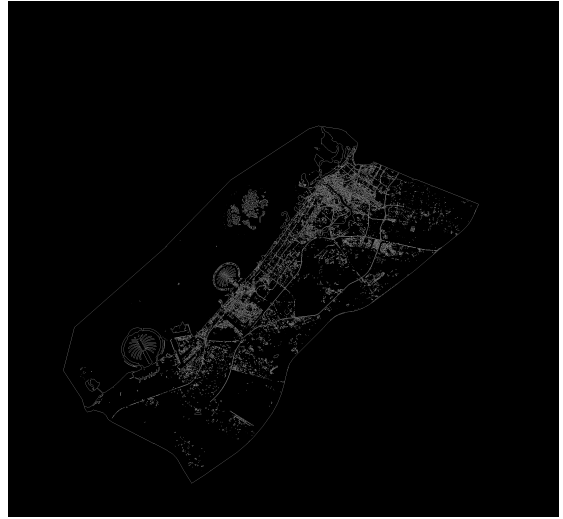


Figure 9: L-8 OLI Image (2016) edge detection

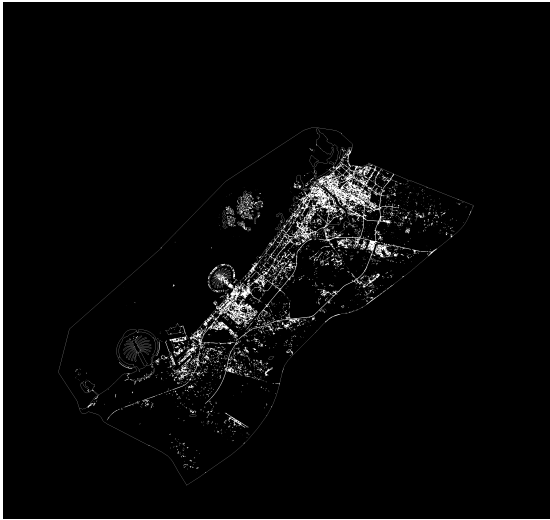


Figure 10: L-8 OLI Image (2016) morph. closing



Figure 11: L-8 OLI Image (2016) eroded

were equalised to have comparable images.

The different image segments (e.g. vegetation, water, land) were then classified using supervised classification and the kNN-algorithm. For this, reference RGB values had to be taken of the different desired classes to build a database for reference classes. This was done manually and the database then embedded in the MATLAB Code for the classification. For the purpose of this report only the results of the *water-class* are used. The algorithm was then run on the masked, cropped and equalised images (fig. 7). Two example results can be seen in figs. 12 and 13.

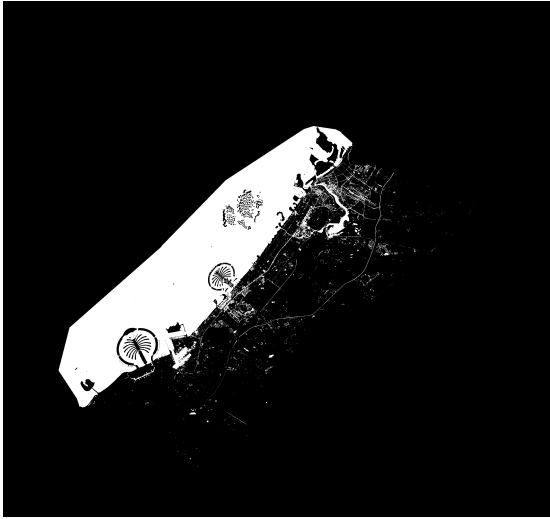


Figure 12: L-8 OLI Image (2016) water class

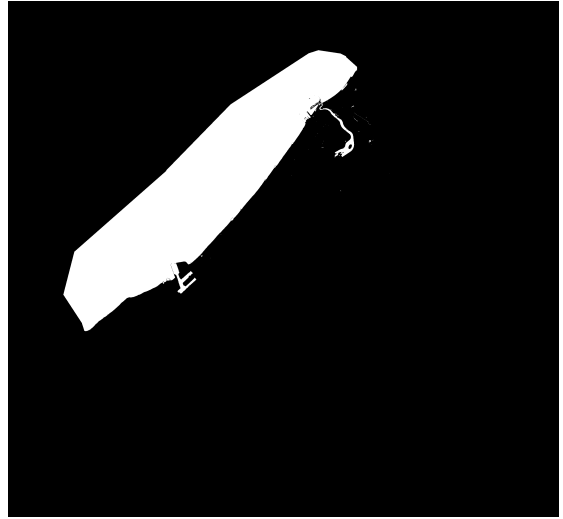


Figure 13: L-5 TM Image (1984) water class

The water area could then also be calculated by simply summing the binary image.

5 Discussion

After processing the image as explained in the previous chapter, the relative relation inbetween the pictures could be presented with the summed binary image data for both techniques. The result is shown in figs. 14 and 15.

One can observe that there are quite high variations in some parts of the water analysis. This is due to failures or insufficient processing, e.g. Image 7 (1990) has a weird cutoff in the northern part, which results in a lower detection of water particles. Unfortunately, the exact reason for this could not be found.

Also, the Images taken with LandSat-8 include some streets and other ground areas that are falsely classified as water by the kNN algorithm. A reason for this might be the histogram equalisation. As can be seen in fig. 7, some of the streets appear blue/violet. It is not clear why exactly this happens - since it only occurs on the LandSat-8 data. A cause might be the "sharper" image of the LandSat-8 satellite, due to technology improvements and better satellite stabilisation or the difference between the captured visible spectral bands, since the LandSat-8 OLI has a lower wavelength range compared to the others. This could lead to a different colour profile, and thus an incorrect histogram equalisation.

But also the analysis using the edge detection has some drawbacks. The edge detection of course detects edges regardless if it's e.g. a border between land and water or a street and water.

However, plotting the trendline in the results (figs. 14 and 15) shows that the initial hypothe-

ses can be confirmed, since the trend line for the water detection decreases, thus the water abundance is lower in later years, and the structure, and thus street and house availability increases

Comparing this to officially available demographic data the analysis seems to be qualitatively correct, since the population has been growing since the

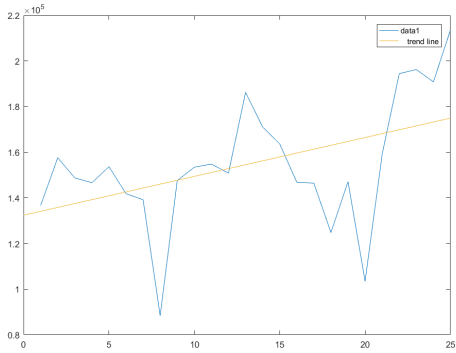


Figure 14: street detection with trend line

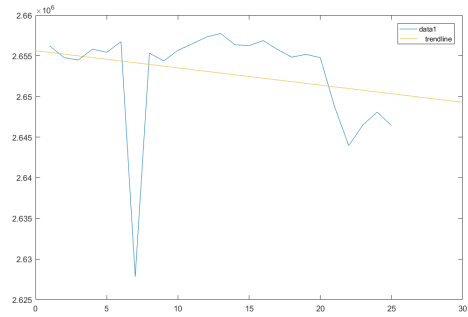


Figure 15: water detection with trend line

6 Conclusion

As stated in the introductory part of this report, Dubai is a very fast growing and expanding city, mainly due to its initially vast oil resources and thus its attraction and accumulation of wealth and wealthy people.

This was expected to lead to an increase in infrastructure development, due to the increasing population. Based on these assumptions, two hypotheses were made concerning the expected landscape change in satellite imagery.

These hypotheses were examined using LandSat image data starting from the year 1984 until the year 2016. However, due to technical reasons, the limited scope of this report and the unavailability of data for unknown reasons there exist gaps in the data between 2003 to 2008 and 2008 to 2013.

Finally, using two different approaches, the hypotheses could be qualitatively verified, thus an observation of Dubai's infrastructure using space-based imagery is feasible and possible with basic algorithmic approaches.

However, since the used algorithmic approach is only basic it could be optimised by a lot, e.g. doing a better classification of water, land and streets and use a better approach for the edge detection than just apply morphological closing to detect the area.

Also, in further work one could fill the data gaps with image data provided by other satellites. Another also promising approach would be to use an extended image histogram equalisation, since the spectral bands used to create the data differed throughout the used imagery. Further

research should be done to show if there is an approach to account for this issue.

For a more accurate result, one could also take into account the classification of vegetation and streets. A quick glance on the data (created during the kNN classification), showed that the vegetation and streets were classified quite accurate in some images. Still, for this report this data was not used, due to limited time and resources.

It would also be interesting to create or use an approach that would allow automatic masking and cropping images (which was done manually for this report), for example using overlay-algorithms to detect the best mask fit between two images.

To conclude, the overall approach to observe infrastructure development from space seemed feasible, even on a very basic level, thus it might be interesting to improve this approach by optimising the algorithms and fill the existing gaps in data with more satellite images in further work.

The whole Appendix including MATLAB Code, Images and Report-Latex file can be downloaded from the following githug-repository:

<https://github.com/art1/UE52-Earth-Observation-Report>

For the sake of completeness and to ease referencing, the MATLAB Code is also given within this report in the following Appendix A.

A MATLAB Code

A.1 ROI Selection and Histogram Equalisation

```

1 clear all; close all; clc;
2 % This
3
4
5 %% crop images to only contain ROI (experimentally determined)
6 roi = [ 2350    220    3200    3000];
7 srcfiles = dir('imagedata/alldata/*.png');
8 for i = 1 : length(srcfiles)
9     filename = strcat('imagedata/alldata/',srcfiles(i).name);
10    I = imread(filename);
11    I2 = imcrop(I,roi);
12    [pathstr,name,ext] = fileparts(filename);
13    imwrite(I2,strcat('imagedata/alldata/',name,'cropped',ext));
14 end
15
16 %% equalize histogram for the images
17 srcfiles = dir('imagedata/alldata/*cropped.png');
18 % use 1992 as reference image
19 ref = imread('imagedata/alldata/1992cropped.png');
20 for i = 1 : length(srcfiles)
21     filename = strcat('imagedata/alldata/',srcfiles(i).name);
22     I = imread(filename);
23     I2 = imhistmatch(I,ref);
24     % mask the image with the original image again
25     mask = rgb2gray(I);
26     mask = (mask > 0.001);
27     mask(:,:,2) = mask;
28     mask(:,:,3) = mask(:,:,1);
29     I2 = immultiply(mask,I2);
30     [pathstr,name,ext] = fileparts(filename);

```

```

31   imwrite(I2 , strcat( 'imagedata/alldata/' ,name , '_refd' ,ext)) ;
32 end

```

A.2 Edge Detection

```

1 clear all; close all; clc;
2
3
4 %% run an edge detection on cropped images and calculate
5 % structure area.
6
7 srcfiles = dir('imagedata/alldata/*cropped_refd.png');
8 R = zeros(1,length(srcfiles), 'uint32');
9 for i = 1 : length(srcfiles)
10   filename = strcat('imagedata/alldata/' ,srcfiles(i).name);
11   X = imread(filename);
12   % convert to grayscale
13   BW1 = rgb2gray(X);
14   % do some fancy edge detection (use the standard one! Canny
15   % produces not useful data!)
16   BW2 = edge(BW1);
17
18   % do some morphological closing to get outlined area
19   BW3 = bwmorph(BW2, 'close',30);
20   % erode the image to get rid of the border we don't want
21   BWer = bwmorph(BW1, 'erode',1);
22   BWermask = BWer.*BW3;
23   % close again, just to surely get the max area
24   BWermask = bwmorph(BWermask, 'close',Inf);
25   % plot one of each image from the last data set for the report
26   if i == length(srcfiles)
27     [pathstr ,name ,ext] = fileparts(filename);
28     imwrite(BW1,strcat('imagedata/analysis/street' ,name ,
29     '_grayscale' ,ext));
30     imwrite(BW2,strcat('imagedata/analysis/street' ,name , '_edge' ,
31     ext));
32     imwrite(BW3,strcat('imagedata/analysis/street' ,name , '_close' ,
33     ext));
34     imwrite(BWer,strcat('imagedata/analysis/street' ,name , '_erode' ,
35     ext));
36   end
37   % now reshape and count pixels

```

```

33 [r col] = size(BWermask);
34 BW_resh = reshape(BWermask, 1, r*col);
35 cnt = 0;
36 figure;
37 imshow(BWermask);
38 for j=1:length(BW_resh)
39     if BW_resh(j) > 0.4
40         cnt = cnt +1;
41     end
42 end
43 % write image, obviously
44 [pathstr, name, ext] = fileparts(filename);
45 imwrite(BWermask, strcat('imagedata/analysis/street', name, ext));
46 % append it to a matrix
47 R(i) = cnt;
48 end
49
50 % plot the data
51 figure, plot(R)

```

A.3 Colour Analysis

```

1 clear all; close all; clc;
2
3 % this file runs a kNN algorithm using pre-set classes (manually
done)
4
5 srcfiles = dir('imagedata/alldata/*cropped_refd.png');
6
7 R = zeros(1, length(srcfiles), 'uint32');
8 for i = 1 : length(srcfiles)
9     filename = strcat('imagedata/alldata/', srcfiles(i).name);
10    I = imread(filename);
11    X = I;
12    % supervised classification using kNN algorithm
13    [U,V,d] = size(I) ;
14    I = double(I) ;
15    DataBase = [ 32 49 57 1 ;
16                 32 49 61 1 ;
17                 36 53 61 1 ;
18                 32 51 61 1 ;
19                 36 53 57 1 ;

```

```

20      45 61 69 1 ;
21      40 57 65 1 ;
22      32 45 57 1 ;
23      36 49 61 1 ;
24      32 49 57 1 ;
25      178 162 146 2;
26      182 166 154 2;
27      178 162 159 2;
28      182 162 146 2;
29      121 154 85 3;
30      142 162 101 3;
31      125 158 93 3;
32      125 150 98 3;] ;

33
34
35 NbData = size(DataBase, 1) ;
36
37 Pixels = DataBase(:,1:3) ;
38
39 Classes = DataBase(:,4) ;
40
41 MaskClasses = zeros(U,V) ;
42
43 for u = 1 : U
44     for v = 1 : V
45
46         r = I(u,v,1) ;
47         g = I(u,v,2) ;
48         b = I(u,v,3) ;
49
50         TabRGB = repmat([r g b],NbData,1) ;
51         D2 = (TabRGB - Pixels).^2 ;
52         % minimise distance
53         [valmin, posmin] = min( sum(D2') ) ;
54         MaskClasses(u,v) = Classes(posmin) ;
55
56
57     end
58 end
59 % plot the water classe, for this report the others aren't used.
60 show = (MaskClasses==1);
61 bordermask = bwmorph(rgb2gray(I), 'erode', 1);

```

```

62     show = show .* bordermask ;
63     show (:,:,2) = show ;
64     show (:,:,3) = show (:,:,1) ;
65     waterMasked = show .* I ;
66     figure ,
67     subplot (1,2,1) ,imshow (X)
68     subplot (1,2,2) ,imshow (show .* I)
69     [pathstr ,name ,ext] = fileparts (filename) ;
70     imwrite (show .* I ,strcat ('imagedata/analysis/water' ,name , '_w' ,ext))
71           );
72
73     % now reshape and count pixels
74     [r col] = size (waterMasked) ;
75     BW_resh = reshape (waterMasked ,1 ,r * col) ;
76     cnt = 0 ;
77     %figure ;
78     %subplot (1,2,1) ,imshow (BWermask) ;
79     %subplot (1,2,2) , imshow (X2) ;
80     for j=1:length (BW_resh)
81         if BW_resh (j) > 0.4
82             cnt = cnt +1;
83         end
84     end
85     % append it to a matrix
86     R (i) = cnt ;
87
88 plot (R)

```

B LandSat Image Data

All the used LandSat Image Data can be downloaded using the following identifiers as input for the *Bulk Download Application* provided on the USGS Website

LC81600432016352LGN00
 LC81600432015269LGN00
 LC81600422015269LGN00
 LC81600432014154LGN00
 LC81600422014154LGN00
 LC81600432013151LGN00
 LC81600422013151LGN00
 LE71600432010279ASN00

LT51600432008138KHC01
LE71600432003148ASN00
LE71600432002273SGS01
LE71600432001190EDC00
LE71600432000188SGS00
LE71600431999265SGS01
LT51600431998286XXX01
LT51600431997011ISP00
LT51600431996345ISP00
LT51600431995278ISP00
LT51600431994179ISP00
LT51600431993160ISP00
LT41600431992166XXX02
LT51600431991171ISP00
LT41600431990240XXX03
LT51600431989165ISP00
LT41600431988027XXX03
LT51600431987272XXX10
LT51600431986045XXX05
LT51600431985042AAA04
LT51600431984136XXX12

References

- Wikipedia Dubai. Dubai wikipedia article, 2017-03-03. URL <https://en.wikipedia.org/wiki/Dubai>.
- USGS Earth Explorer. Usgs online tool for data selection and access to publicly available earth observation satellite data, 2017-03-02. URL <https://earthexplorer.usgs.gov>.
- Google Maps. Image obtained from google maps, using the keyword "dubai", 2017-03-02. URL en.wikipedia.org/wiki/Landsat_4.
- USGS. Haystack: Electronic noise calibrator for the small radio telescope, 2017-03-01a. URL <https://pubs.er.usgs.gov/publication/fs20153081>.
- USGS. Haystack: Electronic noise calibrator for the small radio telescope, 2017-03-01b. URL <https://remotesensing.usgs.gov/index.php>.
- USGS. Landsat-4 history, 2017-03-02a. URL <https://landsat.usgs.gov/landsat-4-history>.
- USGS. Landsat-5 history, 2017-03-02b. URL <https://landsat.usgs.gov/landsat-5-history>.
- USGS. Landsat-7 history, 2017-03-02c. URL <https://landsat.usgs.gov/landsat-7-history>.
- Wikipedia. Landsat-4 article, 2017-03-02. URL en.wikipedia.org/wiki/Landsat_4.